MEASUREMENT OF IN SITU PROTEIN CONCENTRATIONS IN LYMPHATIC CAPILLARIES BY ULTRASOFT X-RAY MICROSCOPY

by

HORACE HILLMAN WATERS

Submitted in Partial Fulfillment
of the Requirements for the
Degree of Bachelor of Science
at the

MASSACHUSETTS INSTITUTE OF TECHNOLOGY

August, 1969

Signature of Author .....
Department of Biology; August 18, 1969

Certified by .....
Thesis Supervisor

Accepted by .....
Chairman, Departmental Committee on Theses

Acknowledgements

It is a great pleasure to acknowledge my deep indebtedness, both personal and scientific, to John F. Burke, M.D., Chief of Staff, Shriners' Burns Institute, Boston Unit, for providing laboratory space, moral and financial support, and a rewarding association over the past two years.

My heartfelt thanks go to Blanca Lusetti and Susan Graves for their ability to produce frozen sections at a moment's notice, to Juanito Billote, M.D., for his valuable histology lessons, and to Miss Alice Scholz, who has provided data on protein concentrations in normal guinea pig serum. To all the other staff of Dr. Burke's laboratory,who have provided an environment in which it has been a distinct pleasure to work, I offer my thanks.

I am deeply indebted to Carl Miller for his skillful microdensitometry.

Special thanks must go to Alan Perelson for his help in calculating the systematic errors and for my introduction to the field of ultrasoft x-ray microscopy.

I am most appreciative of Miss Nancy Wilson's dexterity on the electric typewriter.

Finally, my loving thanks to Heather Anne, who, without realizing it, makes it all worthwhile.

August, 1969

Horace H. Waters

Cambridge, Massachusetts

Table of Contents

Abstract

Thin, freeze-dried sections of guinea pig ear mounted on high resolution photographic emulsion (Kodak high resolution plates) were exposed to ultrasoft x-rays (wavelengths from 19 to 30 Angstroms) in order to measure protein concentrations in small blood vessels, lymphatics, and interstitial spaces. The details of appropriate exposure times and fabrication of the reference system were experimentally determined. Measurement of the optical density of extremely small areas of the photographic emulsion was accomplished by microdensitometry. The geometry of the x-ray tube and sample chamber made it necessary to find a material which would reflect visible light generated by the filament but which would transmit the ultrasoft x-rays. The window was constructed from an aluminized thin film of parylene C (Union Carbide, Bound Brook, N.J.). In situ measurements of protein concentrations in the small blood vessels of normal guinea pig ears were in good agreement with bulk measurements of protein concentrations in normal guinea pig blood. Suggestions were made for further investigation of protein concentrations in abnormal tissue using ultrasoft x-ray microscopy.

Introduction

The x-ray absorption characteristics of small biological structures have been under investigation since 1913 when Goby (1) published x-ray pictures of Foraminifera. His work was limited by the fact that only rather coarse-grained photographic emulsions were available at that time. Dauvillier (2) built equipment capable of producing soft x-rays and used fine grain emulsion resolving about a thousand lines per millimeter to make x-ray absorption pictures of samples placed in a chamber filled with hydrogen gas to reduce absorption of the soft x-rays by air. The mass absorption coefficients of both nitrogen and oxygen are nearly two orders of magnitude greater than the mass absorption coefficient of hydrogen throughout the entire soft x-ray region (3). In the late 1930's, Lamarque (4) used an evacuated x-ray tube and sample chamber to make what he called "historadiographs" of animal tissues. He filtered out visible light generated at the cathode with a thin window of metallic lithium. More recently, Engstrom and Lindstrom (5) have done a thorough theoretical analysis of the problem of soft x-ray absorption in small biological objects. They solved the problem of filtering visible light produced at the cathode with an aluminum foil window nine (9) microns thick. Lindstrom (3) has calculated the systematic errors in determining the dry mass of protein by x-ray absorption techniques. In 1963 Friberg and Burke (6) described an automated soft x-ray instrument capable of sequentially irradiating twelve samples mounted on 1" x 3" slides. The instrument utilizes a highly sensitive transistor circuit to control emission current and a motor driven variable transformer to control

anode voltage. It can be programmed for exposure times ranging from a few minutes to two hours. In 1967 Perelson (7) calculated the "optimal conditions for ultrasoft x-ray microscopy of proteins" for this instrument. The present work is an experimental outgrowth from his theoretical considerations.

The motivation for this investigation has been the illucidation of the mechanism by which proteins move from blood capillaries through interstitial spaces and return to the circulatory system via the lymphatic system. An understanding of this mechanism will help the biologist to study an organism's response to infection, thermal burns, or other large surface wounds. Essential to the successful treatment of a massive thermal burn is the immediate restoration and continuing maintenance of the patient's normal fluid balance (8). A necessary first step toward this understanding is the ability to measure protein concentrations <u>in situ</u> in biological tissue.

Several mechanisms have been proposed for the movement of proteins across capillary walls. Landis and Pappenheimer (9) suggested the existence of small pores in the capillary wall. Grotte (10) and Mayerson (11) have gone one step further and added the possibility of large pores through which proteins might pass. Chambers and Zweifach (12) and Zweifach (13) postulated that these pores could be some kind of permeable "cement" between the cells of the capillary wall. Palade (14) suggested pinocytosis, transport through cells in membrane vesicles, as a possible mechanism for protein movement across capillary walls.

Moore and Ruska (15) proposed "cytopempsis" as a more descriptive name for this process. Leak and Burke (16) have used electron micrographs to demonstrate the existence of two pathways for colloidal particles to gain entrance to lymphatic capillaries; "(1) across the intercellular cleft of patent junction and (2) across the lymphatic endothelium within pinocytotic vesicles."

Ultrasoft x-ray microscopy has been the beneficiary of relatively recent technological advances in several fields. Now, commercially available fine grain photographic emulsion of high definition makes it possible to obtain resolution of more than 2000 lines per millimeter (17). With new diffusion pump fluids routine production of vacua in the 10^{-8} torr range is no longer difficult. Modern microtomes and sectioning techniques have made it possible to produce thin (less than 20 microns) sections of frozen biological tissue with minimal disturbance to tissue structure (18). The technology associated with x-ray photography of solar activity has produced the thin aluminized film presently being used to filter out visible light generated at the cathode of the x-ray tube.

The present investigation is based on the superb pioneering work, both theoretical and experimental, done by Arne Engstrom and Bo Lindstrom in the 1940's and 1950's. The method requires thin sections of biological tissue, in this case 10 and 16 micron sections of guinea pig ears. This material was chosen because it is easy to obtain and because it has well defined vascular and lymphatic systems.

Rapid freezing of the ear after excision and freeze-drying after sectioning preserves the structural features of the material and maintains the distribution of materials in the body fluids. The sections are mounted directly on the photographic emulsion and exposed to ultrasoft x-rays. The high resolution of the emulsion used allows determination of mass density at intervals of 1 to 2 microns. Measurement of the optical density of extremely small areas of the x-ray image was accomplished by microdensitometry techniques described by Miller, Parsons, and Kofsky (19) and Kofsky (20).

Ultrasoft x-ray microscopy has been used to determine total dry weight in tissue structures that are 20 to 35% dry substance by Brattgard and Hyden (21), Engstrom, et al. (22, 23, 24, 25) and Hedberg (26). As far as the author has been able to determine, the present investigation is the first time this method has been used to determine protein concentrations as low as 4 to 7 grams per 100 milliliters, which is the range of concentrations found in blood vessels, lymphatics, and interstitial spaces.

I. Preparation of the Sample

Guinea pigs were sacrificed by a sharp blow to the head. The ears were excised, immediately frozen between two blocks of dry ice and depilated with a razor blade. Small blocks (2-3 cm. x 1 cm.) of ear tissue were mounted for sectioning on the Harris cryostat microtome. Section thicknesses ranging from 10 microns to 16 microns were used in this study. These thicknesses represent a compromise of two variables; (1) mechanical strength of the section, and (2) ability to image structures within the section. Sections thinner than 10 microns are extremely difficult to handle without damaging them. Structural features tend to be obscured or piled on top of one another in sections thicker than 16 microns. The sections were mounted on photographic plates (Kodak high resolution plages, 1" x 3"), which have previously been dipped in a ¼% solution of parlodion in absolute alcohol and ethyl ether (1v: 1v). Perelson (7) determined that the thin coat of parlodion over the emulsion facilitated removal of the tissue and was invisible to the ultrasoft x-rays. Naturally, all the operations involving the photographic plates were carried out in a darkroom under safelights. The mounted sections were freeze-dried for two hours at about 0.02 torr, then stored at room temperature over anhydrous calcium sulfate. After exposure to x-rays the sections were removed from the plate simply by immersion in acetone for 10 minutes. The sections were then mounted on a microscope slide and

stained with hematoxylin and eosin and saved for histological examination and comparison with the x-ray image.

II. Preparation of the Reference System

Lindstrom (3) has described the use of a parlodion reference to quantize protein mass determinations by soft x-ray microscopy. The reference system used in the present investigation was essentially the same as Lindstrom's. The differences were that thinner reference steps were necessary to correspond to the lower concentrations of protein being measured and that the reference system was mounted on a metal frame fixed to lie close to the photographic plate in the x-ray instrument while the tissue was mounted directly on the plate. The latter arrangement allowed the exposure of many different tissue sections with the same reference system. The determination of protein concentrations by x-ray microscopy requires correlation of the optical density of the x-ray image of the tissue with the optical density of the x-ray image of the reference system. The criteria for a good reference system are: (1) it must be easily made into a uniform, thin film, (2) it must be mechanically strong enough to withstand the small amount of handling necessary to mount it on a metal frame, (3) its mass per unit area must be easily determined, and (4) its mass absorption coefficient in the ultrasoft x-ray region must be known. Parlodion fulfills all of these criteria.

1.000 gram of parlodion was dissolved in 100 milliliters each of absolute alcohol and ethyl ether. Microscope slides were

dipped once into this solution and allowed to dry in air at room temperature. The slides were then placed on a microscope stage one at a time in order to cut rectangular strips of accurately known dimensions out of the center of the film. The strips were cut in adjacent pairs; one used in the reference system and one used to gravimetrically determine the mass per unit area. The strips were floated off the slide by slowly immersing it in warm water (50° C.). The reference step wedge was made by sequentially picking up strips of the same width but decreasing length on a metal frame. The strips to be weighed were picked up in preweighed aluminum weighing boats, dried in vacuo over anhydrous calcium sulfate, and weighed on a Cahn electrobalance. The mass per unit area determined by this method was 32.5 micrograms per square centimeter. Uniformity of the thickness of the strips was determined by the uniformity of their color in reflected light while they were floating on surface of the water. The adequacy of this method was confirmed by the uniformity of the optical density of the x-ray image of each step in the reference system.

III. Exposure to X-rays

Throughout this work the author uses the terminology for x-rays proposed by Engstrom (27). Wavelengths below 0.1 Angstroms are termed ultrahard x-rays; 0.1 to 1.0 Angstroms, hard; 1.0 to 10.0 Angstroms, soft; and above 10.0 Angstroms, ultrasoft. Most of the work mentioned in the historical introduction was done in the soft x-ray region, while the present work was done in the ultrasoft region. This imposes more stringent requirements on the vacuum system used since both oxygen and nitrogen absorb heavily in this region (3). Operating vacua were normally near 10^{-7} torr in the x-ray tube and sample chamber, which requires a vacuum system capable of at least 10^{-8} torr when blanked off. The system used was a six-inch oil diffusion pump with a hand-operated high vacuum valve supplied by the Norton Company, Palo Alto, California, backed by a 160 liters per minute Welch mechanical pump. The high vacuum valve allowed the isolation of the x-ray tube and sample chamber from the diffusion pump permitting rapid attainment of operating vacua after changing samples. The x-ray tube was a Model Z-146 supplied by the Dunlee Corporation, Bellwood, Illinois. The tube employed a tungsten target with an effective spot size of 1.5 x 1.8 millimeters. For a section thickness of 10 microns the geometrical unsharpness was less than 0.2 micron at target-to-plate distance of 6 inches (6). The cathode

was demountable for ease of filament replacement. Both the cathode and the anode were water cooled.

A major problem in ultrasoft x-ray microscopy was the inherent inefficiency of the tube. The normal operating point was an anode voltage of 650 volts and an emission current of 30 milliamperes. Under these operating conditions the filament produces large quantities of visible light. The classical solution to this problem in the soft x-ray region has been to use a window of thin (5 to 10 microns) aluminum or lithium foil. For ultrasoft x-rays a much thinner window was necessary. A double thickness of 0.7-micron aluminum foil was used but it proved to be unsatisfactory because it was mechanically very delicate, extremely difficult to handle without damage, and not consistently uniform in thickness. A second generation window was made by vacuum deposition of a thin coat (approximately 0.06 microns) of aluminum on a thin film of VYNS-3 resin (Union Carbide Plastics Company, New York, N.Y.), a polyvinylchloride-acetate copolymer described by Pate and Yaffe (28). The window was a sandwich of two pieces of coated film with the aluminum in the middle. This was discarded because the x-ray absorption characteristics of the film were unknown, the film disintegrated under prolonged x-irradiation, and adequate control of the thickness of the aluminum coating could not be maintained from one batch to the next. It was learned that American Science and Engineering, Inc., Cambridge, Mass. had solved a similar problem in taking x-ray pictures of the sun (29). The material they used was

an aluminum-coated film of parylene C (Union Carbide Corporation, Bound Brook, N.J.). An aluminized (0.12 microns of aluminum on each side) pellicle (0.5 microns thick) of parylene C was obtained and made into windows. A double thickness of this material proved to be light-tight, extremely uniform, easy to handle, and stable to x-irradiation. An x-ray transmission curve for parylene C in the ultrasoft region was obtained (30).

Perelson (7) calculated the optimum wavelength, for the tissue section thickness used and for use of the parlodion reference system, to be 23 Angstroms. In the ultrasoft region the tube generates a continuous spectrum (Figure 1) independent of the target material. The minimum wavelength of the continuous spectrum is determined by the anode voltage, v, (31)

$$\lambda_o = 12.4/v \qquad (1)$$

where λ_o is in Angstroms and v is in kilovolts. The intensity distribution is that for a thin target where maximum intensity occurs at the minimum wavelength and thereafter the intensity falls off as $1/\lambda^2$. At an anode voltage of 650 volts the minimum wavelength is 19 Angstroms. This operating point was chosen to eliminate the longer wavelengths which are a source of large systematic errors and to produce a reasonable intensity at the optimum wavelength of 23 Angstroms. At this operating point the aluminized parylene C window effectively eliminates all wavelengths greater than 30 Angstroms (Figure 1).

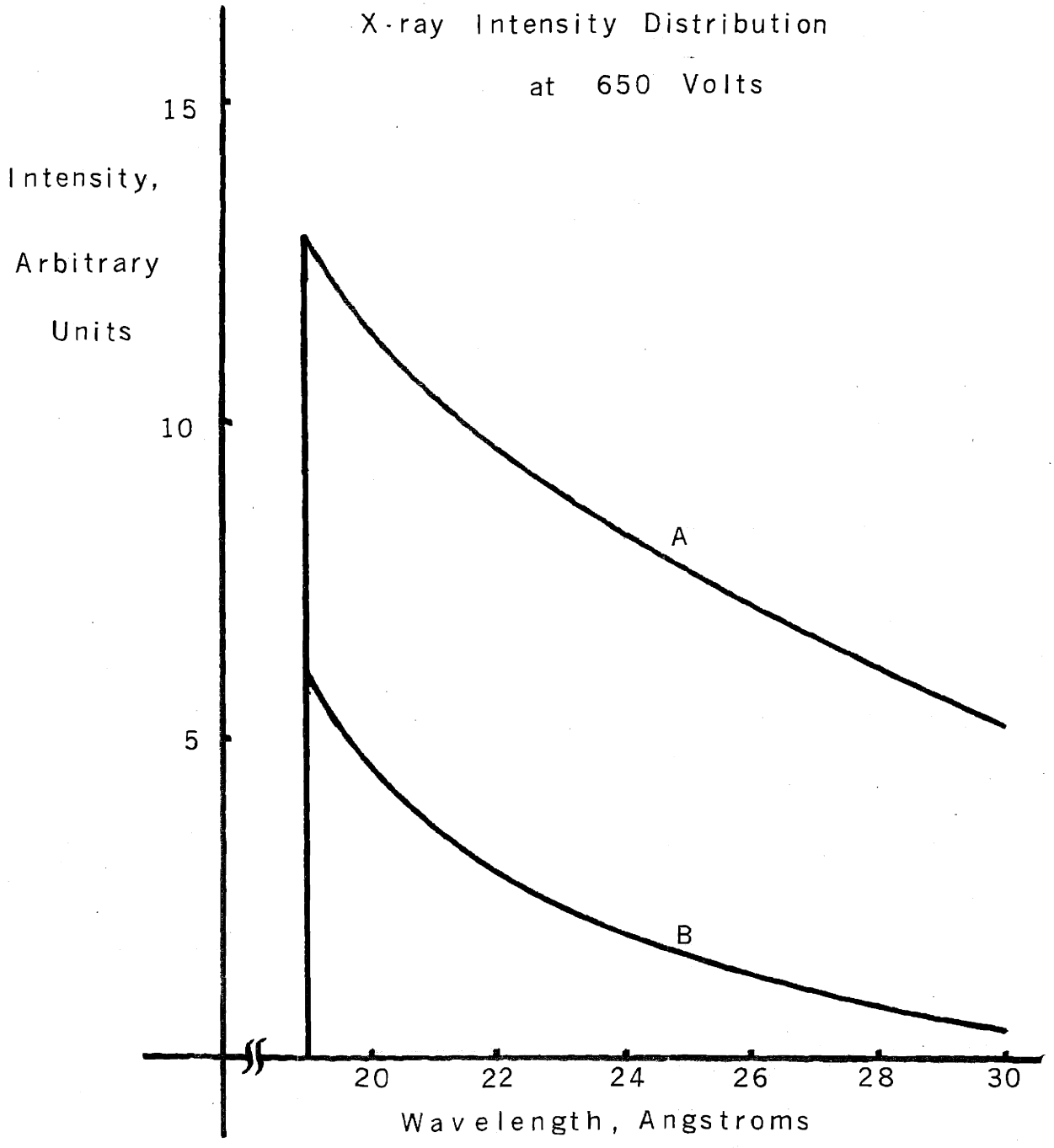

Figure 1. Continuous Spectrum of X-ray Intensity Produced by Anode Voltage of 650 Volts.
Curve A is the spectrum produced by the x-ray tube.
Curve B is the spectrum after filtering through the aluminized parylene C window.

With an emission current of 30 milliamperes the exposure time for good definition and contrast of the x-ray image was experimentally determined to be approximately 45 minutes. Exposure times ranging from 20 to 60 minutes have been used to produce acceptable results. Perelson (7) found a slight increase in efficiency of x-ray production during the first hour of operation of the instrument. The author almost completely eliminated this variable by leaving the power supplies constantly turned on when the instrument was being used regularly.

After exposure to x-rays, removal of the parlodion coating, and demounting of the tissue, the plates were developed in Kodak HRP developer for 10 minutes, stopped in Kodak indicator stop bath for 30 seconds, fixed in Kodak fixer for 10 minutes, washed in tap water for 30 minutes, rinsed with distilled water, and treated with Kodak Photo-flo 600 (diluted 600:1 with distilled water) for 30 seconds. All the above operations were carried out at 68°F with continuous agitation. All photochemicals were made up with distilled water.

IV. Microdensitometry

The x-ray image of the tissue on the photographic emulsion was examined microscopically. Blood vessels and lymphatics were located by comparison of the x-ray image with the stained tissue section that was removed from the x-ray plate. Small arteries were rather easy to locate in the x-ray image due to their relatively thick walls which absorbed all or nearly all of the incident x-irradiation (cf. Figures 2, 5 and 6). Veins were slightly more difficult to identify but with practice it became relatively simple to pick them out. Lymphatics presented a difficult identification problem due to the loose structure of their walls and the very low concentration of protein in the lumena. For this reason, lymphatics which were in close proximity to easily identifiable blood vessels were selected (cf. Figures 5 and 6). Polaroid photomicrographs were made of the x-ray images of structures whose densities would be measured. This was done to allow identification of images when the x-ray slide was placed on the microdensitometer. Two dimensional contour maps of the optical density of the x-ray images of blood vessels, lymphatics, and reference wedges were made by Carl Miller (Photometrics, Inc., Lexington, Mass.) on a Technical Operations Isodensitracer (Technical Operations, Inc., Burlington, Mass.). The Isodensitracer (microdensitometer) and the theory of its operation has been described by Kofsky (20). Figure 2 is the contour map of the optical density of the x-ray image of a small artery and its associated reference wedge; Figure 3, a small vein and its wedge;

and Figure 4, a lymphatic and its wedge. Figure 5 is a photomicrograph of the stained tissue showing these three structures in close proximity. Figure 6 is a photomicrograph of the x-ray image of the same three structures. Figures 2, 3, 5 and 6 illustrate one of the difficulties of this method. Both the vein and the artery are partially filled with red blood cells (see Figure 5). These are so dense that they absorb all of the incident x-irradiation making measurements of these areas impossible. The red blood cells correspond to the dark areas inside the vessels in Figure 5, the light gray areas inside the vessels in Figure 6, and the red-lined areas inside the vessels in Figures 2 and 3. It is possible to select small areas free of blood cells within the vessels and calculate protein concentrations with reasonable accuracy. Figure 7 is the contour map of the optical density of the x-ray image of a small blood vessel and its associated step wedge. Figure 8 is a photomicrograph of the stained tissue showing this vessel, and Figure 9 is a photomicrograph of the x-ray image of this vessel. This vessel is very close to the ideal case since it contains only a single blood cell, the dark spot near the right center of the bottom edge of the vessel lumen in Figure 8, which can easily be disregarded when calculating the protein concentration.

Perelson (7) determined that the optical density of the developed photographic emulsion is a linear function of its exposure to ultrasoft x-rays in the range of densities encountered in the

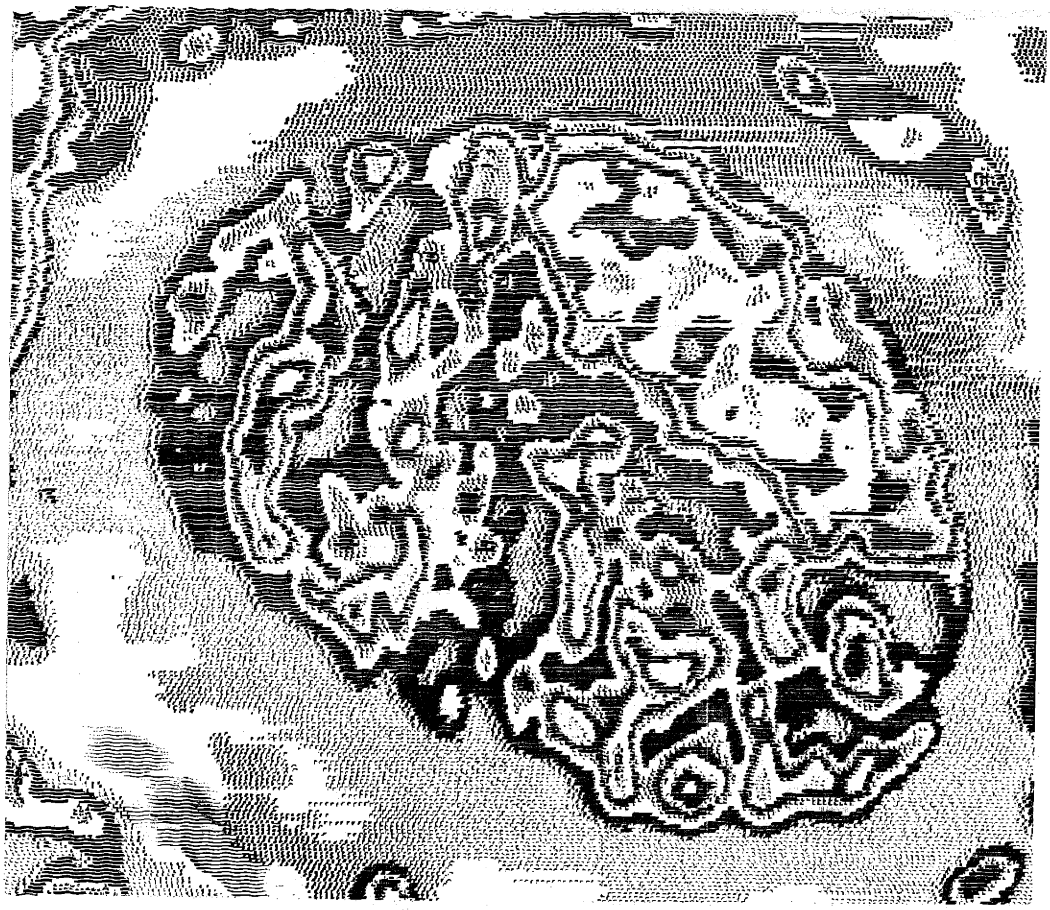

(a)

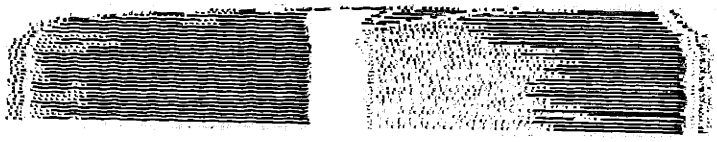

(b)

Figure 2. (a) Contour Map of Optical Density of X-ray Image of Small Artery in Guinea Pig Ear.

The inside boundary of the arterial wall is represented by the large, roughly elliptical boundary between red dots and red lines; this is the zero level of x-ray exposure. Moving in toward the center of the area thus defined,red lines represent areas of high concentration (red blood cells as explained in the text); boundary of green dots and green lines represent areas with the same absorption as three thicknesses of the reference wedge; white space between green lines and blue dots, two thicknesses; blue lines, one thickness; and red dots surrounded by blue lines, zero level of reference wedge (opposite end of scale from zero level of x-ray exposure). Magnification: x 850.

(b) Contour Map of Optical Density of X-ray Image of Reference Wedge.

Green dots and lines correspond to three thicknesses of the wedge; white space between green lines and blue dots, two thicknesses; red lines and dots, zero level. The single thickness if present would be blue lines.

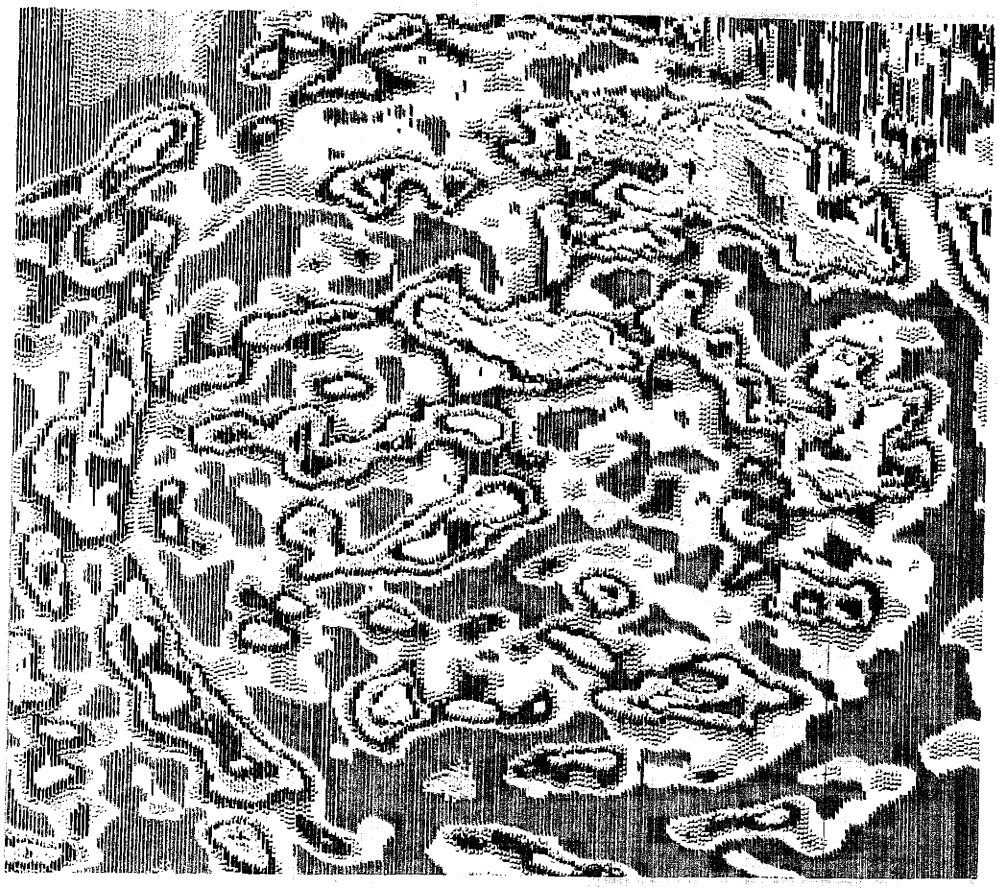

(a)

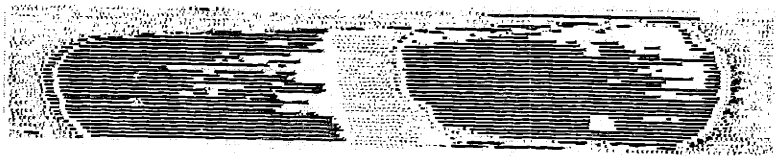

(b)

Figure 3. (a) Contour Map of Optical Density of X-ray Image of Small Vein in Guinea Pig Ear.

The boundary of the vein is difficult to discern but is identifiable by the practiced eye. Similar to Figure 2, green lines represent three thicknesses of the reference wedge; blue dots, two; white space between blue lines and red dots, one; and red lines, zero level. Magnification: x 850.

(b) Contour Map of Optical Density of X-ray Image of Reference Wedge.

As above, green lines are three thicknesses; blue dots, two; red lines, zero level. Single thickness if present would be white space between blue lines and red dots.

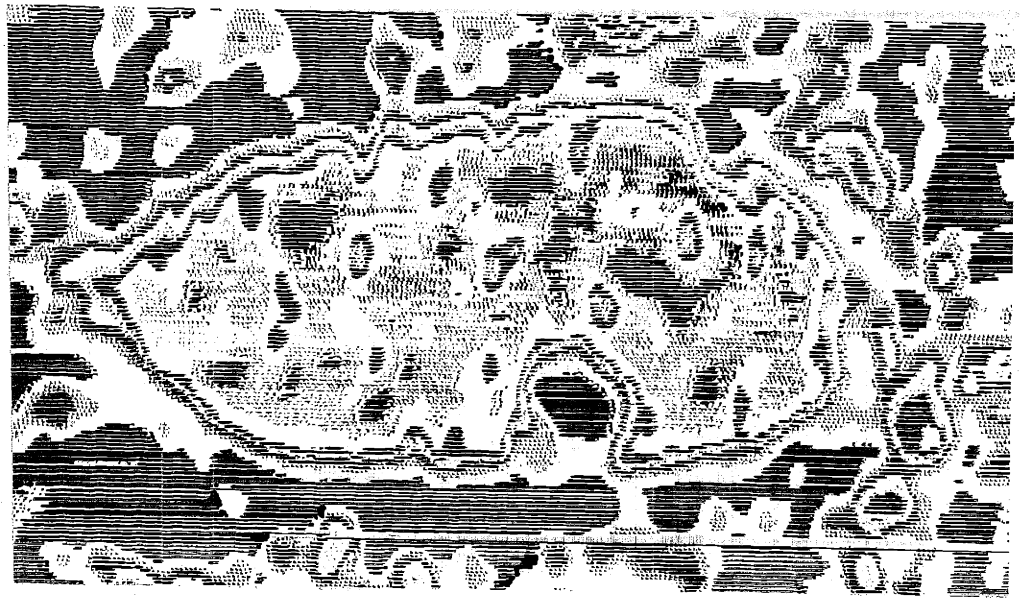

(a)

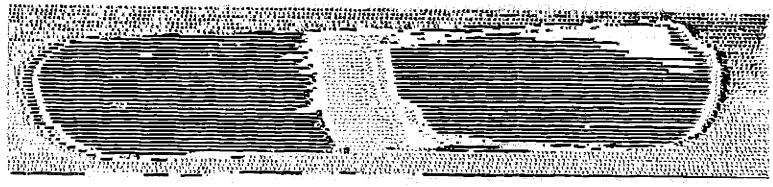

(b)

Figure 4. (a) Contour Map of Optical Density of X-ray Image of Lymphatic in Guinea Pig Ear.
Calibration is identical to that of Figure 3(a).
Magnification: x 850.

(b) Contour Map of Optical Density of X-ray Image of Reference Wedge.
Identical to Figure 3(b).

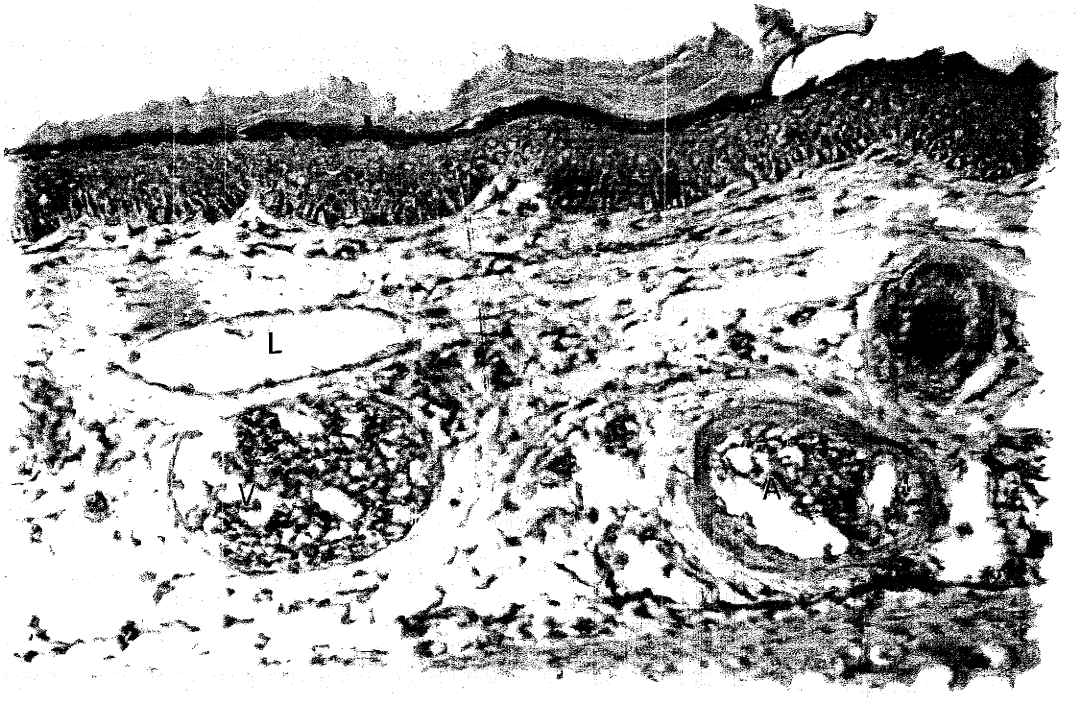

Figure 5. Photomicrograph of Hematoxylin-and-Eosin-stained Tissue.

A is the artery of Figure 2, V is the vein of Figure 3, and L is the lymphatic of Figure 4. Magnification: x 200.

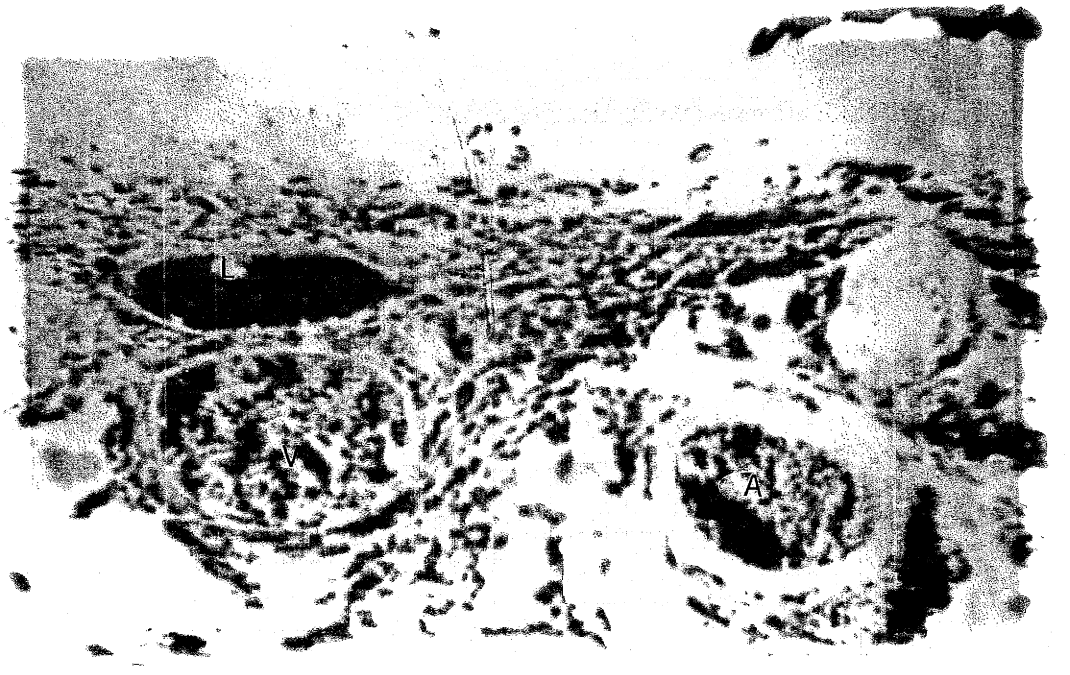

Figure 6. Photomicrograph of X-ray Image of Thin Section of Guinea Pig Ear.

A is the artery of Figure 2; V is the vein of Figure 3; and L is the lymphatic of Figure 4. Magnification: x 200.

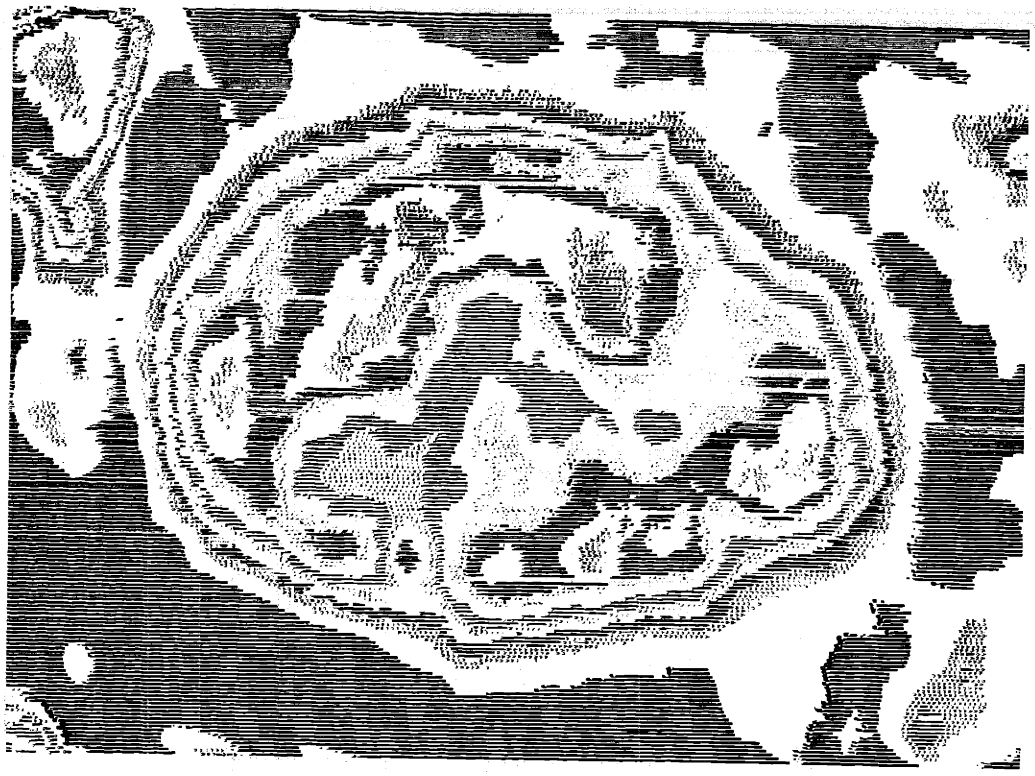

(a)

(b)

Figure 7. (a) Contour Map of Optical Density of X-ray Image of Small Blood Vessel in Guinea Pig Ear.

Nearly elliptical configuration of red dots and lines corresponds to vessel wall; green dots, three thicknesses of wedge; green lines, two; blue dots, one; and blue lines, zero level. Magnification: x 850.

(b) Contour Map of Optical Density of X-ray Image of Reference Wedge.

Calibration as in 7(a) above.

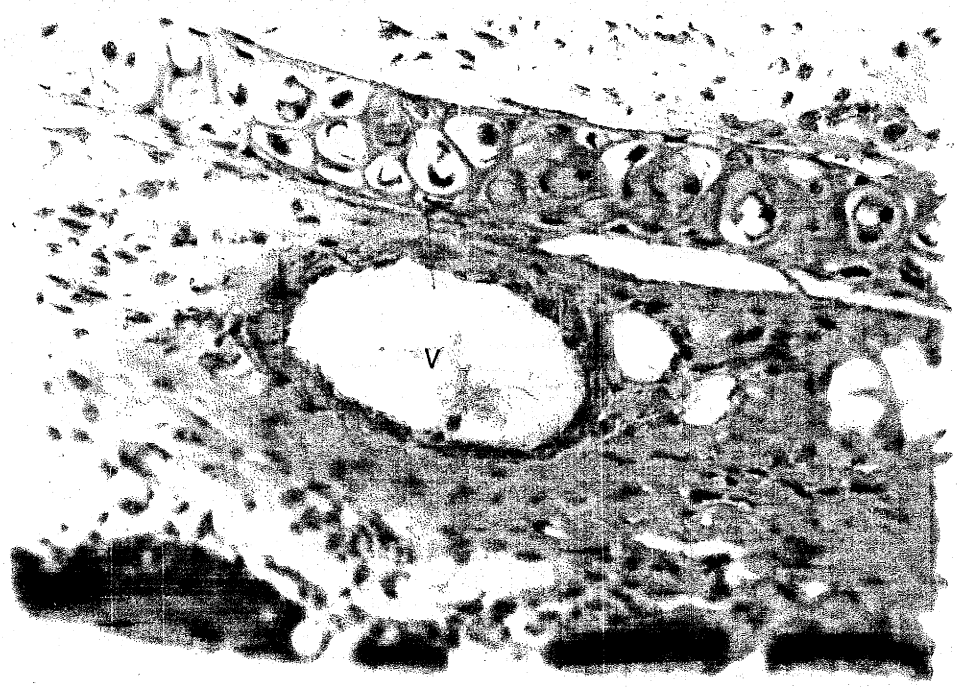

Figure 8. Photomicrograph of Hematoxylin-and-Eosin-stained Thin Section of Guinea Pig Ear.

V is the blood vessel of Figure 7. Magnification: x 280.

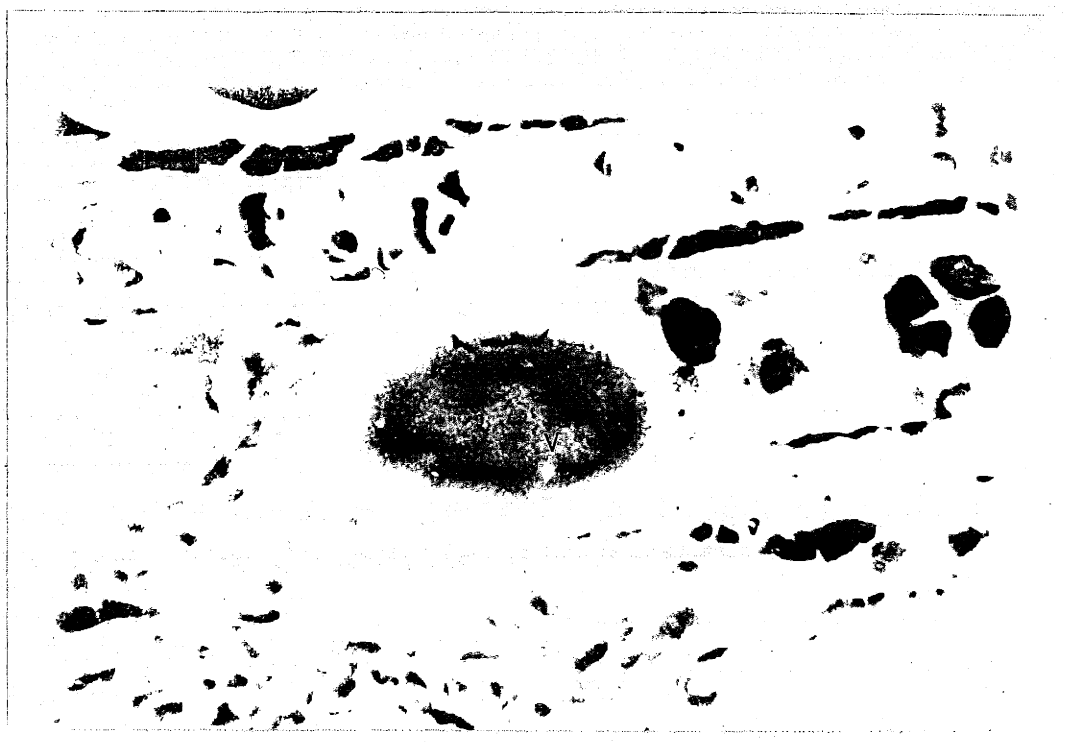

Figure 9. Photomicrograph of X-ray Image of Thin Section of Guinea Pig Ear.

V is the vessel of Figure 7. Magnification: x 280.

in the present investigation. This enables a direct correlation of optical densities with mass per unit area by relating contour lines in the map of the wedge to contour lines in the map of the blood vessel. In this way, levels of the reference wedge with the same absorption as that of the tissue structure can be identified. Since the mass per unit area of each level of the reference wedge is known, the mass per unit area of the tissue structure can be calculated by the following equation from Lindstrom (3):

$$(1 + \epsilon)\, m_x = m_{ref} \frac{\sum_{j=1}^{n_1} I_{oj} \left(\mu/\rho\right)_{ref_j}}{\sum_{j=1}^{n_1} I_{oj} \left(\mu/\rho\right)_{prot_j}} \qquad (2)$$

where ϵ = the systematic error due to the presence of constituents other than protein in the tissue

m_x = mass per unit area of protein

m_{ref} = mass per unit area of reference system

the x-ray spectrum is divided up into n_1 regions, each of mean wavelength, λ_j

I_{oj} = intensity of the jth region

$(\mu/\rho)_{ref_j}$ = mass absorption coefficient of the reference system at λ_j

$(\mu/\rho)_{prot_j}$ = mass absorption coefficient of protein at λ_j

This is equivalent to the equation

$$(1 + \epsilon)\, m_x = m_{ref} \frac{\sum_{j=1}^{n_1} I_{oj} \frac{(\mu/\rho)_{ref_j}}{(\mu/\rho)_{prot_j}}}{\sum_{j=1}^{n_2} I_{oj}} \qquad (3)$$

used by the author to calculate mass per unit area of protein in tissue structures. Perelson (32) has written a computer program which calculates ϵ based on the composition of guinea pig blood given in Table 1. The program was written before transmission data for the window (cf. P. 14 above) was available and includes wavelengths up to 44 Angstroms. The filtering effects of the window on high wavelengths is shown by curve B of Figure 1. The author has used the output of Perelson's program to recalculate ϵ by hand excluding all wavelengths above 30 Angstroms. The same program also calculates the weighted ratio (see Equation 3 above) of the mass absorption coefficients of parlodion and protein, based on the ratios given in Table 2. The author has recalculated this ratio by hand excluding all wavelengths above 30 Angstroms. These calculated values reduce Equation 3 to

$$(1 - 0.168)\, m_x = 0.92\, m_{ref} \qquad (4)$$

or simply

$$m_x = 1.10\, m_{ref} \,. \qquad (5)$$

Since the mass per unit area of the parlodion film used to make the reference wedge was 32.5 micrograms per square centimeter, one thickness of the reference wedge corresponds to a protein mass per unit area of 35.8 micrograms per square centimeter. Dividing by the thickness of the tissue in centimeters and multiplying by 10^{-6} grams per microgram and 100 cubic centimeters per 100 milliliters gives the protein concentration in grams per 100 milliliters. For 10-micron

Table 1

Composition of Guinea Pig Blood (33)

Substance	Concentration (mg/100 ml)
Protein (34)	5000.0
Calcium	10.7
Chloride	361.0
Magnesium	2.3
Potassium	25.3
Sodium	320.0
Sulfate	3.3
Phosphate	5.3
Glycine	2.5
Lipid	169.0
Glucose	155.0
Pyruvate	2.3
Choline	7.0
TOTAL	6063.7

Table 2

The Ratio of the Mass Absorption Coefficient of Parlodion to that of Protein (32)

Wavelength (Angstroms)	MAC Parlodion/MAC Protein
19	1.295
20	1.284
21	1.273
22	1.269
23	0.627
24	0.624
25	0.625
26	0.625
27	0.622
28	0.623
29	0.625
30	0.625

sections, one thickness of the reference wedge corresponds to a protein concentration of 3.58 grams per 100 milliliters. Since protein does not dry in a uniform layer inside the blood vessel, this concentration varies widely over the cross-sectional area of the vessel as is evident from the contour maps in Figures 2, 3, 4 and 7. In order to average these measured concentrations, tracing paper was placed over the contour maps, the outline of the vessel and the contour lines were traced, the outline was cut out and weighed, and areas corresponding to different concentrations were cut out and weighed. From these weights it was possible to calculate the average value of the protein concentration in the section of blood vessel. This is extremely tedious work and the source of a small but indeterminate amount of error. The possibility of putting the optical density information on computer tape and computing averages by machine is being explored.

ERRATUM

Page 33. Sentence 4 should read "Calculated values of protein concentrations, 5.1 grams per 100 milliliters for the artery of Figure 2; 5.4 grams per 100 milliliters for the vein of Figure 3; 1.9 grams per 100 milliliters for the lymphatic of Figure 4; and 4.8 grams per 100 milliliters for the blood vessel of Figure 7, were in good agreement with values obtained independently."

V. Results

The purpose of this investigation was to measure protein concentrations in small blood vessels and lymphatics of the guinea pig ear by ultrasoft x-ray microscopy. Several problems standing in the way of these measurements were experimentally solved. For example, a suitable material, aluminized parylene C, was found to filter out visible light and transmit ultrasoft x-rays, construction of a reference wedge of the appropriate thickness for the range of concentrations encountered was accomplished, proper exposure times were determined, and a tedious but serviceable means of averaging protein concentrations, measured at points within a structure, over the area of that structure. Calculated values of protein concentrations, 5.1 grams per 100 milliliters for the artery of Figure 2; 5.4 grams per 100 milliliters for the lymphatic of Figure 4; and 4.8 grams per 100 milliliters for the blood vessel of Figure 7, were in good agreement with values obtained independently. Miss Alice Scholz (34) has determined the protein concentration of normal guinea pig serum to be 5.00 grams per 100 milliliters. Chemical analysis (35) of a sample of the same serum yielded a protein concentration of 4.6 grams per 100 milliliters. No data is available on the concentration of protein in guinea pig lymphatics. The agreement of measurements of protein concentrations in blood vessels by ultrasoft x-ray microscopy with measurements by other methods

indicates that some confidence can be placed in the values obtained by ultrasoft x-ray microscopy for protein concentrations in lymphatics.

This study has been limited to normal tissue by the amount of available time and by delays caused by various mechanical failures of equipment. The x-ray tube had to be replaced, once because the target had become etched by long use, and a second time when it cracked due to a failure of the cooling system. The vacuum system was entirely replaced at one point causing a long delay in operations.

There are many experiments suggested by the success of this investigation. Some knowledge about the mobility of proteins when an organism responds to infection, burning, or other insult may be obtained through measuring protein concentrations by ultrasoft x-ray microscopy of infected or burned tissue. The method can be applied to many systems other than the guinea pig ear. The success of this investigation gives the biologist a valuable tool for making in situ measurements of protein concentrations at very low levels.

References

1. Goby, P. "Micro-Radiography," Arch. Roentgen Ray, London, 18 (1913), p. 247-250.

2. Dauvillier, A. "Realisation de la microradiographeie integrale," Compt. rend., 190 (1930), p. 1287-1289.

3. Lindstrom, B., "Roentgen Absorption Spectrophotometry in Quantitative Cytochemistry," Acta Radiol., Suppl. 125 (1955).

4. Lamarque, P., "Historadiography; A New Application of X-rays," Radiology, 27 (1936), p. 563-568.

5. Engstrom, A. and B. Lindstrom, "A New Method for Determining the Weight of Cellular Structures," Nature, 163 (1949), p. 563-564.

6. Friberg, U. and J. F. Burke, "Automation in Microradiography," in Pattee, H.H., V.E. Cosslett, and A. Engstrom, X-ray Optics and X-ray Microanalysis, New York, Academic Press, 1963.

7. Perelson, A. Unpublished Undergraduate Thesis, Department of Electrical Engineering, Massachusetts Institute of Technology, 1967.

8. Burke, J.F., "Present Clinical Aspects of Burns -- A Symposium," IIIrd Yugoslav Congress for Plastic and Maxillofacial Surgery with International Participation, Maribor, May, 1968.

9. Landis, E.M. and J.R. Pappenheimer, "Exchange of Substances through the capillary walls," in Handbook of Physiology, Section II, "Circulation" Vol. II, Washington, D.C., American Physiological Society, 1963.

10. Grotte, G., "Passage of dextran molecules across the blood-lymph barrier," Acta Chir. Scand. Suppl. 211, p. 1-84, 1956.

11. Mayerson, H.S., "The physiological importance of lymph," in Handbook of Physiology, Sect. II, "Circulation," Vol. II, Washington, D.C.

12. Chambers, R. and B.W. Zweifach, "Intercellular cement and capillary permeability," Physiol. Rev. 27, p. 436-463, 1947.

13. Zweifach, B.W., "Pathophysiology of the blood vascular barrier," Angiology 13, p. 345-355, 1962.

14. Palade, G.E., "The endoplasmic reticulum," J. Biophys. Biochem. Cytol. 2 (suppl.), p. 85-98, 1956.

15. Moore, D,H, and H. Ruska, "The fine structure od capillaries and small arteries," J. Biophys. Biochem. Cytol. 3, p. 457-462, 1957.

16. Leak, L.V., and J.F. Burke, "Electron microscopic study of lymphatic capillaries in the removal of connective tissue fluids and particulate substances," Lymphology 1, p. 39-52, 1968.

17. Kodak High Resolution Plates, Kodak Pamphlet, p. 47, 1967.

18. Stumpf, W.E., and L.J. Roth, "Freeze-drying of small tissue samples and thin frozen sections below -60°C," J. of Histochem. and Cytochem., 15, p. 243-51, 1967.

19. Miller, C.S., F.G. Parsons, and I.L. Kofsky, "Simplified Two-dimensional Microdensitometry," Nature 202, p. 1196-1200, 1964.

20. Kofsky, I.L., "Reduction of pictorial data by microdensitometry" presented at the Symposium on Aerospace Measurement Techniques held at M.I.T. on 7-8 July 1966.

21. Brattgard, S.-O. and H. Hyden, "Mass, lipids, pentose, nucelo-proteins and proteins determined in nerve cells by x-ray microradiology," Acta Radiol. Suppl. 94 (1952).

22. Engstrom, A. and D. Glick, "The mass of gastric mucosa cells measured by x-ray absorption," Science, 111, p. 379-380, 1950.

23. _____, and Lindstrom B., "A new method for determining the weight of cellular structures," Nature 163, p. 563-564, 1949.

24. _____, and H. Luthy, "The distribution of mass and lipids in the single nerve fiber," Exptl. Cell Research, 1, p. 81-91, 1950.

25. _____, and F. Ruch, "Distribution of mass in salivary gland chromosomes," Proc. Nat. Acad. Sci. U.S. 37, p. 459-461, 1951.

26. Hedberg, E., "The chemical composition of thr human ovarian oocyte," Acta Endocrinol. Suppl. 15 (1953).

27. Engstrom, A., "Contact microradiography: a general survey," in V.E. Cosslett, A. Engstrom, and H.H. Pattee, X-ray Microscopy and Microradiography, New York, Academic Press, 1957.

28. Pate, B.D., and L. Yaffe, "A new material and techniques for the fabrication of very thin films fur use in 4 -counting," Can. J. of Chem. 33 (1955).

29. Miller, C.S., Personal Communication, September, 1968.

30. Spivak, M., Personal Communication, May 7, 1969, Union Carbide, Bound Brook, N.J.

31. Engstrom, A., X-ray Microanalysis in Biology and Medicine, New York, Elsevier, 1962.

32. Perelson, A., Unpublished Computer Program, June 18, 1969.

33. Dittmer, D.S., Blood and other Body Fluids, Washington, D.C., Fed. of Amer. Soc. for Exptl. Biol., 1964.

34. Scholz, A.E., Unpublished data.

35. Burke, J.F., Personal Communication.